ACTA GEOLOGICAHISPANICA, v. 36 (2001), nº 3-4, p. 213-232

Paleoseismological analysis of late Miocene lacustrine successions in the Prebetic Zone, SE Spain

Estudio paleosismológico en sucesiones lacustres del Mioceno superior en la Zona Prebética, SE de España

M.A. RODRÍGUEZ PASCUA[1], G. DE VICENTE[1] and J.P. CALVO[2]

(1) Dpto. Geodinámica, F. CC. Geológicas, Universidad Complutense, 28040 Madrid. mpascua@eucmos.sim.ucm.es y albosque@eucmax.sim.ucm.es
(2) Dpto. Petrología y Geoquímica, F. CC. Geológicas, Universidad Complutense, 28040 Madrid. jpcalvo@eucmax.sim.ucm.es

ABSTRACT

A paleoseismological study of late Miocene lacustrine sediments was carried out in the Neogene basins of the Prebetic Zone in Albacete (Spain). We developed a multidisciplinary methodology which could be used to extrapolate the paleoseismic data to the present day. This multidisciplinary approach includes different disciplines, i.e. stratigraphy, structural analysis, seismological analysis and paleoseismology. Paleoseismological analysis was focussed on both shallow and deep lake deposits given that these sediments behave differently in different deformation fields. The seismites formed in shallow sediments were generated by liquefaction and include: sand dikes, pillow structures and intruded and fractured gravels. The deep lake deposits show varied structures, such as loop bedding, disturbed varved lamination, mixed layers and pseudonodules. Seismites indicate paleoearthquake magnitude intervals. The trends of the seismites are usually oriented very close to the stress field trends (from the late Miocene to the Present): NW-SE and NE-SW trends. This constitutes a link between tectonics and seismites. The varved annual sedimentation evidenced by the deep lake facies was used as a relative dating method. Mixed layers were employed as paleoseismic indicators to calculate the earthquake recurrence interval. The mean recurrence interval is close to 130 years (9446 years of total record with 73 dated events), one maximum interval of 454 years and one minimum interval of 23 years and the mean estimated magnitude value is 5.1. The Gutenberg-Richter relationship shows similar "b" values close to 0.86 from paleoseismological and seismological data. This suggests that the seismic conditions have been similar since the late Miocene.

Keywords: Seismites. Lacustrine deposits. Varved sediments. Tectonics. Stress field. Paleoearthquake recurrence intervals. "b" value.

RESUMEN

El estudio paleosismológico en las cuencas neógenas (Mioceno superior) lacustres del Prebético de Albacete ha sido abordado mediante un enfoque multidisciplinar para poder extrapolar los datos paleosímicos a la actualidad. Dicho enfoque integra las siguientes disciplinas: estratigrafía, análisis estructural, análisis de la sismicidad y paleosismología. El estudio paleosismológico se ha realizado en

depósitos de facies someras y profundas, ya que los sedimentos de ambas zonas presentan un comportamiento diferente frente a la deformación. Las sismitas localizadas en sedimentos someros fueron generadas por fenómenos de licuefacción y son: diques de arena, estructuras en almohadilla y licuefacción y fracturación en gravas. Las zonas profundas presentan estructuras más diversas: *loop bedding*, alteración de la estructura planar de varvas, niveles de mezcla y pseudonódulos. Las sismitas estudiadas se pueden utilizar como indicadores de intervalos de magnitudes sísmicas. Las estructuras se orientan sistemáticamente según los campos de esfuerzo reciente y actual (que se mantienen desde el Mioceno superior hasta la actualidad): NW-SE y NE-SW. Éste es un punto que permite relacionar genéticamente la tectónica y las sismitas. Se ha utilizado el carácter anual de la sedimentación varvada para datar de forma relativa las estructuras y establecer periodos de recurrencia de paleoterremotos. El intervalo de recurrencia medio está próximo a los 130 años (9.446 años de registro total y 73 eventos datados), el intervalo máximo es de 454 años y el mínimo de 23 años y la magnitud media estimada es de 5,1. Se ha aplicado la ley de Gutenberg-Richter a los datos paleosísmicos y de sismicidad actual y se obtienen valores del parámetro "b" muy similares, próximos a 0,86. Todas estas premisas indican que las condiciones de la sismicidad en el Mioceno superior fueron muy similares a las actuales.

Palabras clave: Sismita. Depósitos lacustres. Sedimentos varvados. Tectónica. Campos de esfuerzo. Intervalos de recurrencia de paleoterremotos. Parámetro "b".

INTRODUCTION

One of the main problems of the study of ancient deformational structures is to determine the deformation trigger mechanism (Owen, 1987; Collison, 1994) because different deformation mechanisms can generate similar structures. Paleoseismic studies focussed on the deformational structures seek to resolve this question. Sims (1975) proposed a number of criteria to be met by soft-sediment deformational structures caused by earthquakes. These criteria are based on sedimentological analysis. Accordingly, in this work we developed a multidisciplinary approach to enlarge these criteria by studying the deformational structures in late Miocene lacustrine sediments of the Prebetic area, SE Spain. Moreover, the data obtained by different techniques can facilitate the comparison between paleoseismic data (late Miocene - Quaternary) and present seismic data.

Despite the suitability of lacustrine deposits for paleoseismic studies (Sims, 1975), there have been relatively few investigations to date. Many lacustrine sediments deposited under permanent subaqueous conditions are suitable for liquefaction. This accounts for the good preservation of the paleoseismic deformational structures (seismites, Seilacher, 1969) given that no significant erosion processes take place in this setting. This is especially true when these lakes are deep enough to generate water stratification and to produce accumulation of varve-like sediments under anoxic conditions. Each pair of laminae usually takes a year to form as a result of seasonal variations. This allows dating of the varved sequences and more information on the age of the associated seismites.

GEOGRAPHICAL AND GEOLOGICAL SETTING

The study area is located in the southern part of the province of Albacete (SE Spain). During the late Miocene, a number of continental basins were formed along the boundary between the Iberian chain (NW-SE trending structures) and the northeastern part of the Betic chain (SW-NE trending structures) (Fig. 1), known as the Prebetic Zone (Sanz de Galdeano and Vera, 1992). There are several basins filled with continental successions in the area (Fig. 2). These basins vary in extension, ranging from a few km^2 (Híjar basin) to 250 km^2 (Las Minas basin). The basins are typically elongate and were formed as rapidly subsiding troughs from the late Vallesian to the late Turolian (Elizaga, 1994; Calvo and Elizaga, 1994). During this interval, the basins were filled with continental, mainly lacustrine sedimentary deposits attaining 500 m in thickness. From a structural point of view, this area is located in the Cazorla-Alcaraz-Hellín structural arc (Alvaro et al., 1975). This area is a transfer fault zone, crossed by three main strike-slip dextral faults with NW-SE directions (Fig. 2): Pozohondo, Liétor and Socovos-Calasparra (Martín Velázquez et al., 1998). The Socovos-Calasparra fault separates the Internal Prebetic Zone to the South from the External Prebetic Zone to the North. Both zones show different features of the Mesozoic and pre-Neogene depositional record. The late Miocene basins are bounded by E-W normal faults. Most of the basins, i.e. Las Minas, El Cenajo, Elche de la Sierra show an asymmetrical tectonic pattern as a result of higher activity of the faults which bound the northern basin margins. In contrast, the Híjar basin, located to the South of the Liétor fault, is elongate in a N10E trend and both the western and eastern flanks of the basin are bounded by normal faults which show the same trend (Calvo et al., 1998).

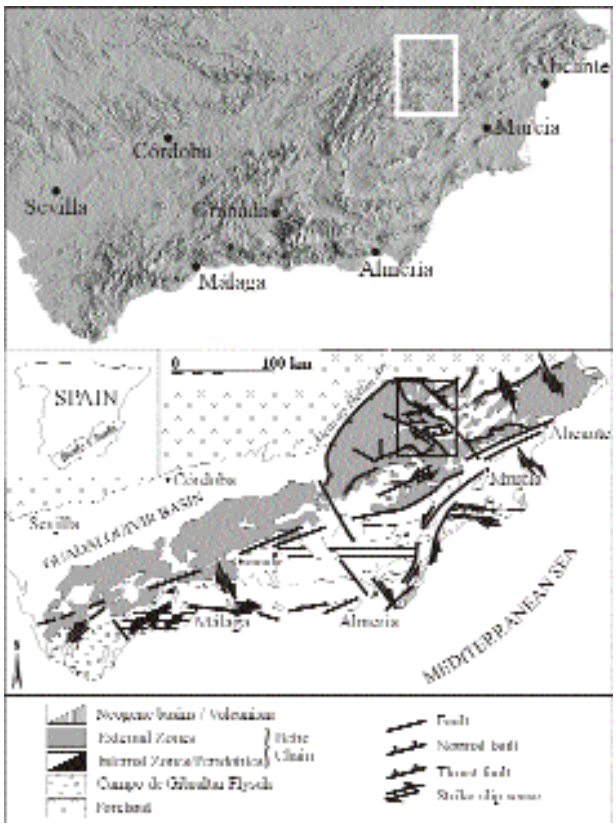

Figure 1. Geographical and geological location of the study area.

Figura 1. Situación geográfica y geológica del área de estudio.

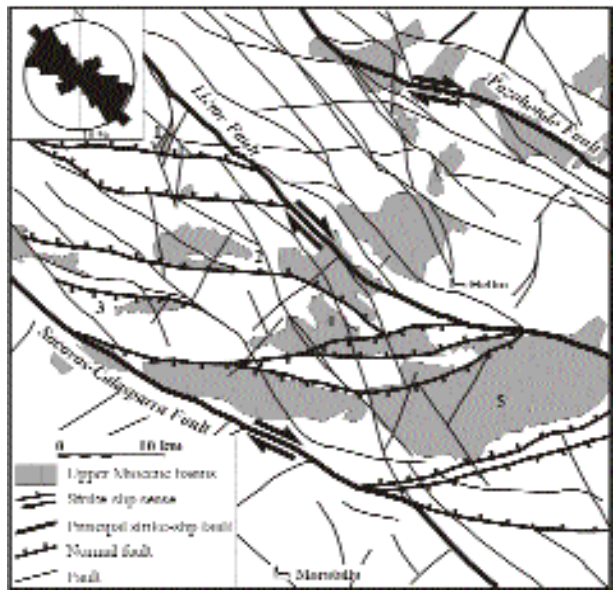

Figure 2. Tectonic framework of the study area. Location of the lacustrine basins developed throughout the late Miocene: 1, Híjar; 2, Elche de la Sierra; 3, Gallego; 4, El Cenajo; 5, Las Minas; in the upper left corner, rose diagram of fault trends.

Figura 2. Esquema tectónico del área de estudio. Localización de las cuencas lacustres desarrolladas durante el Mioceno superior: 1, Híjar; 2, Elche de la Sierra; 3, Gallego; 5, Las Minas; y rosa de direcciones de fallas.

METHODS

One of the main objectives of paleoseismology is to identify recurrence intervals of earthquakes that occurred prior to historical chronicles. This is supported by the identification of seismic deformational structures in sediments (i.e. seismites, Seilacher, 1969). The current technique consists of the detection of faults exposed by trenches, although this methodology only allows us to determine 3 or 4 relatively recent events. Paleoseismic analyses are studies of natural "paleoseismographs", the lacustrine sediments being suitable for this purpose. The annual character of the laminated pairs which make up the sequences allows relative dating of the seismites and the calculation of the recurrence intervals in the stratigraphic record. In many cases, the different types of seismites have been described without establishing a link with the tectonic context in which the seismites developed.

The seismic history of a region can be very well documented for some time intervals. The problem usually lies in applying a suitable methodology that could be used to project information from the past to the present. A multidisciplinary approach involving geology, geophysics and mathematics (Fig. 3) is commonly needed for this purpose:

Stratigraphic analysis

This deals with the characterization of the sedimentary basin fill in which seismites are recognized. This analysis is essential for confirming or ruling out the seismic origin of the deformational structures. In addition, tectonic-sedimentation relationships allow us to improve our understanding of the basin evolution.

Structural analysis

This is based mainly on fault population analysis designed to calculate the recent stress field (late Miocene-Quaternary), which is responsible for the

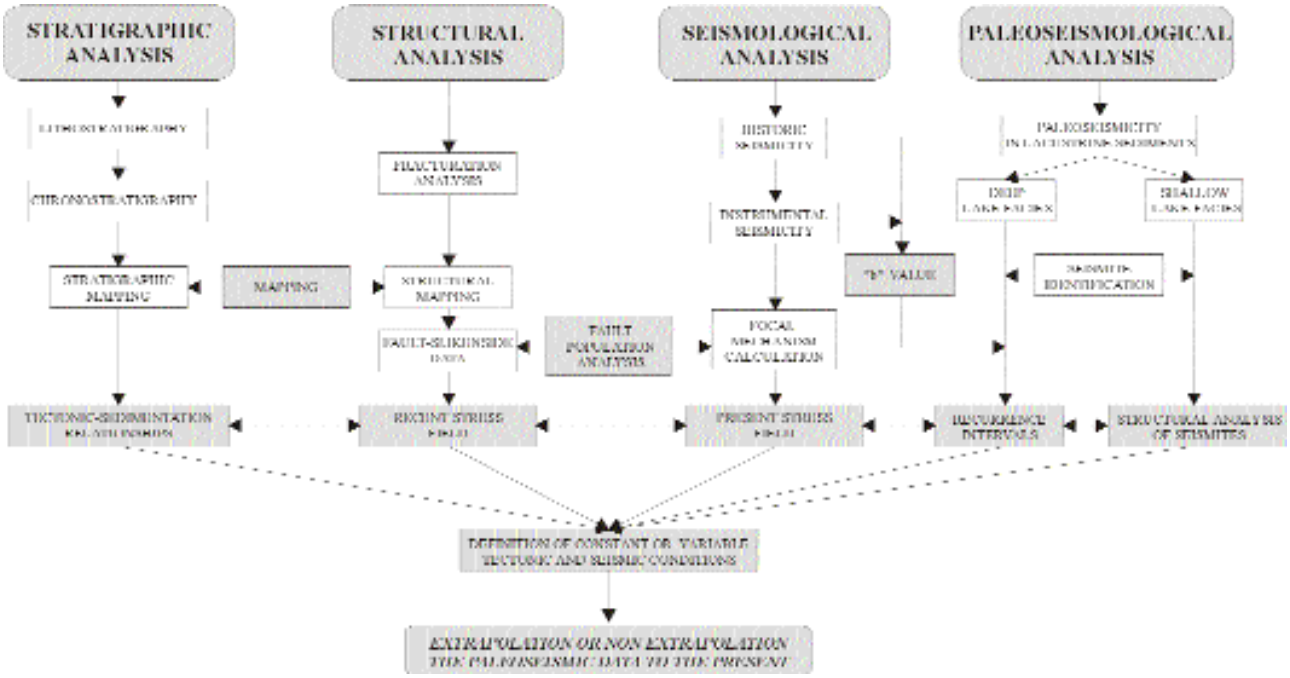

Figure 3. General applied interdisciplinary approach in this work, using different disciplines: sedimentology, structural analysis, seismological analysis and paleoseismology.

Figura 3. Metodología general aplicada en este trabajo, donde se han utilizado las siguientes áreas de conocimiento: sedimentología, análisis estructural, análisis sismológico y paleosismología.

main seismogenetic forces in the area where the basins occur.

Seismological analysis

This is used to calculate the present stress field which can be compared with the stress field evolution of the basin since its formation. Moreover, the study of potential laws, e.g. the Gutenberg-Richter relationship, allows the comparison between the present seismicity of a region and that deduced from paleoseismic analysis.

Paleoseismological analysis

This is based on lacustrine sequences. In these sequences, the distinction between shallow and deep lacustrine facies is meaningful. In shallow lacustrine sequences, the seismites are interpreted as purely tectonic structures in which orientation is directly related to the recent stress field. Deep lacustrine sequences allow, in addition, dating of the seismites and further calculation of the periodicity of earthquakes in the past. Based on these features, potential laws can be applied to deep lacustrine sequences in order to compare paleoseismicity with the present seismicity of the region.

STRATIGRAPHY AND TECTONO-SEDIMENTARY EVOLUTION

The stratigraphic and tectono-sedimentary evolution of the basins studied are described in order to facilitate our understanding of the evolution of the sedimentary systems and their relationship with tectonics. Moreover, this assists in the interpretation of the deformation structures by combining the information on recent and present stress tensors with that furnished by sedimentological data.

The sedimentary fill of the different continental basins in the area shows a similar pattern although the basins were geologically unconnected. The similarities in the vertical evolution of the lacustrine facies are very clear in the Cenajo and Las Minas basins (Fig. 4). The comparison between the stratigraphic successions of the two basins is facilitated by the presence of correlative

beds. Thus, an evaporite unit containing gypsum deposits with native sulphur is observed in both basin infills. Moreover, a set of large-scale slump beds is visible at a similar stratigraphic level (Fig. 4). The latter feature has been interpreted as a result of a high-magnitude seismic event probably related to the extrusion of lamproitic volcanic rocks, dated at 5.7 +/- 0.3 Ma, in the region (Bellon et al., 1981; Elizaga and Calvo, 1988). None of these features occur in the remaining basins (Elche de la Sierra, Híjar, Gallego) although their sedimentary fills show similarities regarding both the thickness and the evolutionary facies pattern trend (Elizaga, 1994).

The lacustrine sedimentary evolution in the Híjar basin is very similar to that of the other Neogene lacustrine basins (Fig. 4). The sedimentary fill in this basin is described as a standard sedimentary continental succession in the Prebetic Zone (Calvo et al., 1978; Elízaga, 1994). The early stages of deposition were characterized by sedimentation of clastic deposits in fan-deltas and/or headed fluvial systems whose source areas are entrenched in the surrounding Mesozoic reliefs. The fluvial sediments are progressively interbedded upwards with palustrine/shallow lacustrine marlstone and carbonate deposits. Further progressive spreading of the lacustrine facies is recorded by marlstone and carbonate deposits. These facies, which are representative of an episode of a relative lake lowstand, are overlain by a thick package of alternating laminated carbonates and marls. The laminated, varve-like marls contain abundant planktonic diatoms and siliceous sponge spicules (Calvo and Elizaga, 1987). Intercalations of carbonate turbidites within the laminated marls are frequent (Fig. 4). Calcareous turbidites can account for up to 70% of the total thickness of the carbonate-marl association (Calvo et al., 1998). These facies characterize an episode of deepening which allows the stratification of the water column and the preservation of the lamination at the lake bottom. The Miocene succession ends with shallow lacustrine marlstones and limestones which gradually pass upward into terrigenous fan-delta facies.

Based on changes observed throughout the stratigraphic successions, the evolutionary history of the basins (obtained in Las Minas basin) can be divided into three main stages (Figs. 5 and 6):

Stage 1

Lacustrine sedimentation was located mainly in the central zone of the basin. Sedimentation was constrained by the Segura strike-slip fault activity and the formation of forced folds. The deposits accumulated in this stage are carbonates, and their deposition followed the formation of the progressive discordance inside the synclinal forced folds. The lowermost deposits that crop out in the Las Minas basin comprise detrital carbonates (turbidites) related to resedimentation from shallow carbonate platforms. The first stage ends with evaporitic sedimentation (gypsum) corresponding to episodes of intense evaporation and extreme shallowness of the lacustrine system, which implies high stability in the basin. The sulfate deposition originated in the early stages of salt tectonic activity (Keuper facies) in some parts of the basin and at the beginning of the extension processes in the region (Fig. 5A).

Stage 2

This stage corresponds to the maximum spreading of the lake system. The active faults were N150E and N060E trending strike-slip faults and normal faults showing an E-W trend. Salt tectonics is favored by activity of the normal faults, especially along the northern border (Los Donceles range). Fan-delta deposits were developed along the northern border, where they evolved distally into turbidites. The north to south transport of clastic deposits is evidence of the intense activity of the normal fault in this basin margin (Fig. 5B).

The south-western margin of the basin was bounded by a normal fault (Monagrillo fault), which constrained the sedimentation in this area. In this sector, the sediment transport was mainly towards the North. This fracture zone constitutes one of the most important limits of the basin, the associated hollow being progressively filled up as the lake expanded (Fig. 5B). Deposition of calcareous turbidites facies characterizes this stage of the generalized deepening of the basin. Lamproitic volcanic rocks (Fuster et al., 1967) of deep origin related to the aforementioned fault were widespread in the basin (Fig. 6A). The southernmost normal fault in the Las Minas basin constrained the sedimentation in this sector. The fluvial transport was toward the North. The monotonous succession of deeper lake deposits includes a slump deposit made up of a set (up to 40 m thick) of contorted and fractured marlstone and limestone beds. This event, which is tentatively related to seismic activity associated with volcanism, leads to the breakdown of the older sediments accumulated in platform and/or basinal areas of the lake.

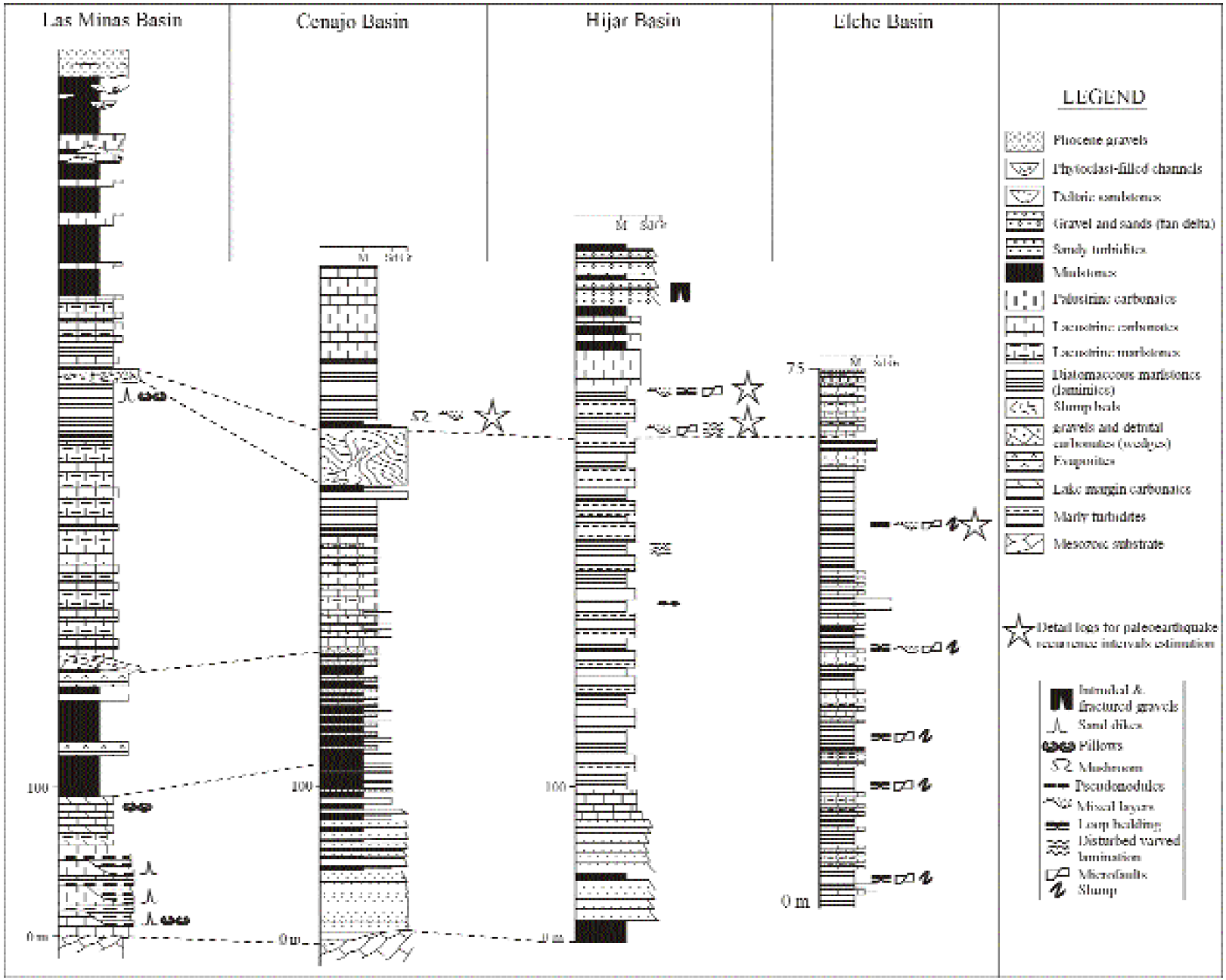
Las Minas Basin
Cenajo Basin
Hijar Basin
Elche Basin
LEGEND
Pliocene gravels
Phytoclast-filled channels
Dolitic sandstones
Gravel and sands (fan delta)
Sandy turbidites
Mudstones
Palustrine carbonates
Lacustrine carbonates
Lacustrine marlstones
Diatomaceous marlstones (laminites)
Slump beds
gravels and detrital carbonates (wedges)
Evaporites
Lake margin carbonates
Marly turbidites
Mesozoic substrate
Detail logs for paleoearthquake recurrence intervals estimation
Intrudial & fractured gravels
Sand dikes
Pillows
Mushroom
Pseudonodules
Mixed layers
Loop bedding
Disturbed varved lamination
Microfaults
Slump
100
0 m
75

The large-scale slump deposit is covered with a thick succession of alternating diatomaceous marlstone and limestone deposited at moderate depth in open lake areas (Bellanca et al., 1989). This succession is also observed in the El Cenajo basin (Fig. 6A).

Stage 3

In this late stage, sedimentation was restricted to the northern part of the basin. The northern normal fault located in the Los Donceles range was active throughout this stage. Fan-delta facies overlying shallow-lake carbonates were observed in this part of the basin. Sediment transport trends were towards NW and SE to the depocenter in the middle part of the basin (Fig. 6B). In the northern part of the Las Minas basin, the Miocene section is capped by a bench-type carbonate along the footwall of the major normal fault that limits the basin margin (Calvo et al., 2000).

STRUCTURAL ANALYSIS. FAULT AND SEISMOLOGICAL ANALYSES

The kinematic and dynamic studies play a major role in determining the seismogenetic sources that generate seismites. The compatibility of the main faults in the area with the stress tensor allows us to deduce which faults were potentially active during the stress field permanency. Likewise, the surface sediments were also affected by stresses which conditioned the genesis of deformational structures. In the case of the seismites, the stress field installed was responsible for the earthquake and the seismite patterns.

Fault population analysis

Paleostress tensors were calculated from 610 striated fault planes, measured in late Miocene-Quaternary rocks, distributed among 23 stations. Different fault population analysis methods were employed to compare the solutions. The stress field was obtained for this time interval. The methods used for the fault population analysis were the following:

- Right dihedra method (Pegoraro, 1972; Angelier and Mechler, 1977).
- Slip model (De Vicente, 1988, based on the Reches model, 1983).
- Stress inversion method (Reches, 1978, 1983, based on the assumption of Bott, 1959).
- Delvaux method (Delvaux et al., 1992; Delvaux, 1993, based on the assumption of Bott, 1959).

After carrying out the fault population analysis and calculating the stress tensor for each station, we elaborated stress trajectory maps for each stress field. The stress trajectories were calculated by the local stress interpolation method, devised by Lee and Angelier (1994) in their TRAJECT program. Thus, we determined the regional stress field evolution that had conditioned the structure of the area from the late Miocene to the Quaternary (Fig. 7A and B).

The solutions obtained (Rodríguez Pascua, 1997, 1998) show two orientations of the maximum horizontal stress (σ_{HMAX}), NW-SE (Fig. 7A) and NE-SW (Fig. 7B). These orientations are mainly obtained by normal faults given that data were collected principally in the extensive basins. The NW-SE orientation is related to the build-up of the structural arc Cazorla-Alcaraz-Hellín, whereas the NE-SW orientation is linked to the formation of the lacustrine basins (which are bounded by E-W normal faults). Both stress fields are simultaneous and the NE-SW trend was generated by the E-W flexural bending of the Betic chain (defined by Van der Beek and Cloething, 1992).

Seismological analysis

Seismicity data were selected depending on the sensitivity of the seismic net of the I.G.N. (Instituto Geográfico Nacional, Spain). Accordingly, the seismic data correspond to a period from 1980 to 1995, which guarantees a good record of earthquakes with magnitudes (M) exceeding 2.7. A total number of 1169 earthquakes were selected with magnitudes higher than this value (maximum magnitude 5.2, mean magnitude 3.2). The selected area is located between 0° and -4° longitude and 40° and 37°

Figure 4. Composite lithostratigraphic logs from the sedimentary fill of the El Cenajo, Híjar and Elche de la Sierra basins. The stratigraphic sketch includes the presence of several types of seismites observed in the lacustrine successions filling the basins and detail logs.

Figura 4. Columnas estratigráficas pertenecientes al relleno sedimentario de las cuencas de Las Minas, El Cenajo, Híjar y Elche de la Sierra. En las columnas se han representado la situación de los diferentes tipos de sismitas observadas y de las columnas de detalle.

latitude, which provides a regional perspective of the seismic phenomenon. It is necessary to recall that the laminate sediments behave as a "paleoseismograph", which records information from distant earthquakes registering a regional seismicity (see the "b" value). The maximum radius in which a liquefaction takes place can exceed 100 km for earthquakes of M>8 (Moretti et al., 1995). Therefore, the area selected for

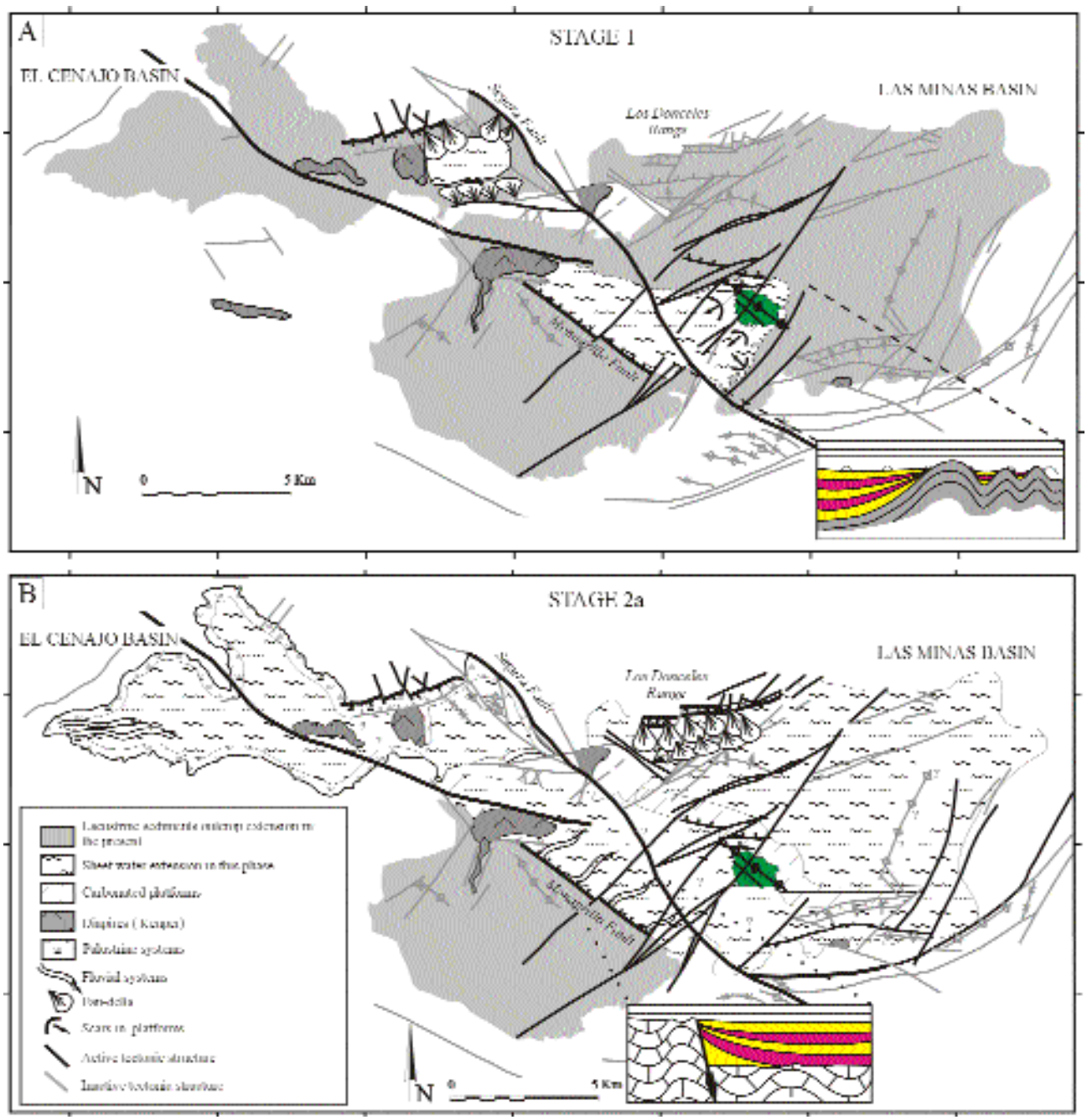

Figure 5. Different sedimentary phases and relationships between the tectonic and the sedimentary phenomena in the Las Minas and El Cenajo basins. A) Stage 1, B) Stage 2a.

Figura 5. Fases sedimentarias y relaciones tectónica-sedimentación en las cuencas de Las Minas y El Cenajo. A) Etapa 1, B) Etapa 2a.

the seismic study contains this constraint. This is the largest area where varved sediments can be used as a "seismograph" by the study of liquefaction structures.

For the analysis of earthquake focal mechanism population, Giner´s method (Giner, 1996) "Pondered Populational Calculation of Earthquake Focal Mechanisms" was used. Twenty eight earthquake focal

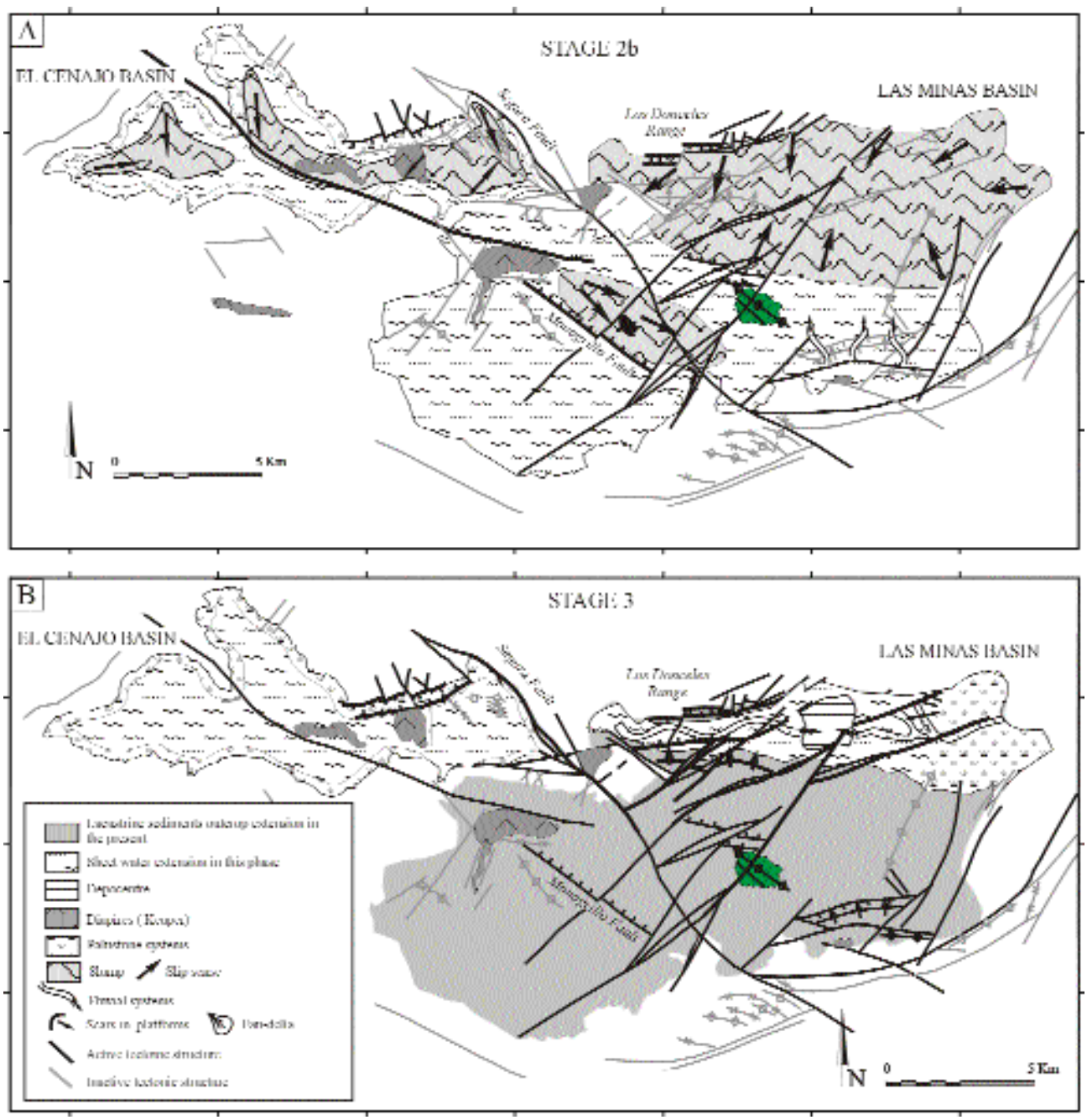

Figure 6. Different sedimentary phases and relationships between the tectonic and the sedimentary phenomena in the Las Minas and El Cenajo basins. A) Stage 2b, B) Stage 3.

Figura 6. Fases sedimentarias y relaciones tectónica-sedimentación en las cuencas de Las Minas y El Cenajo. A) Etapa 2b, B) Etapa 3.

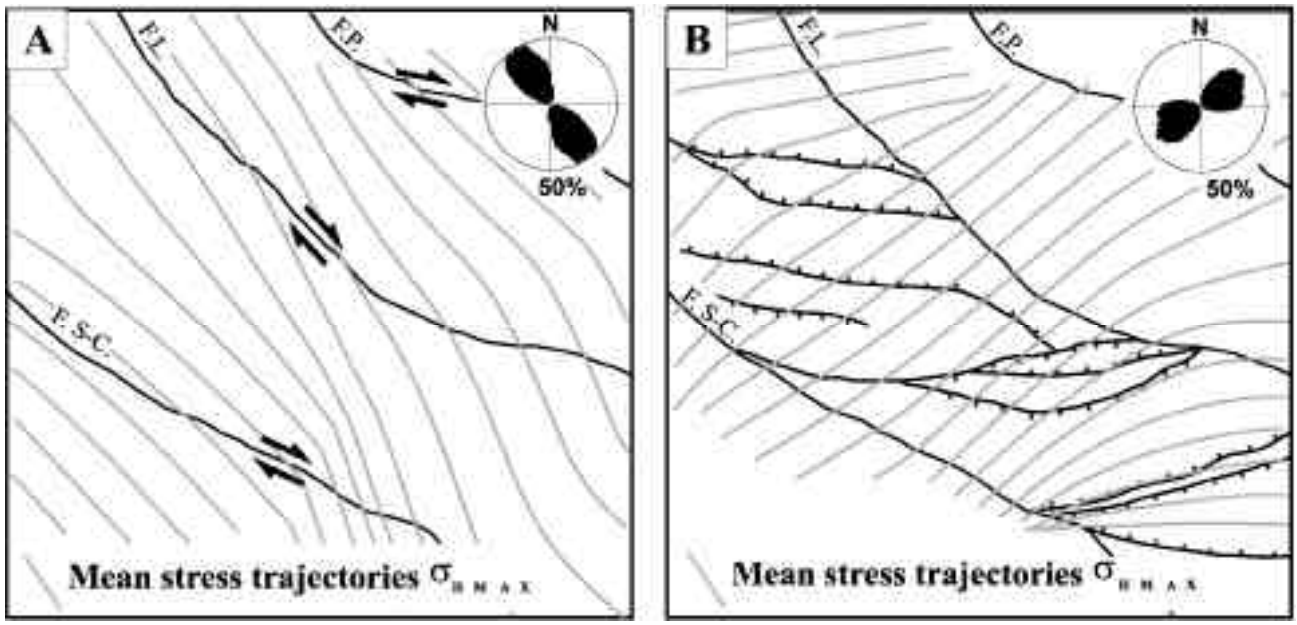

Figure 7. Trajectories of maximum horizontal stress (σ_{HMAX}) calculated by fault population analysis and rose diagram of mean stress trends.

Figura 7. Trayectorias de máximo esfuerzo en la horizontal (σ_{HMAX}) calculadas mediante análisis poblacional de fallas y rosa de direcciones de esfuerzos medios.

mechanisms were calculated and two orientations of maximum horizontal stress (σ_{HMAX}) were obtained: NW-SE and NE-SW (Fig. 8A and B). The NW-SE orientation is defined by reverse faults, whereas the NE-SW is represented by normal faults. These stress fields are coaxial to those inferred from the fault population analysis:

A) Stress field 1 is defined mainly by reverse faults (11 reverse and 3 normal focal mechanisms). The mean σ_{HMAX} shows a N158E trend and the hypocentral depths oscillate between 4 and 22 km (Fig. 8A).

B) Stress field 2 is defined mainly by normal faults (9 normal and 5 reverse focal mechanisms). The mean σ_{HMAX} shows a N062E trend and the hypocenters with normal mechanisms are shallower than those with reverse ones (between 2 and 15 km) (Fig. 8B).

The fact that the normal faults are shallower than the reverse ones has been attributed to the NE-SW flexural bending of the Betic chain. Thus, the reverse faults were generated below the neutral surface of the flexural bending (where compression exists), whereas the normal ones were generated above this surface (where extension exists). The flexural bending was generated by the collision of the African plate against the Iberian microplate, which occurred following a NW-SE orientation, coincident with the calculated NW-SE stress field. The NE-SW orientation corresponds to a secondary stress field generated by surficial extension that took place over the antiformal flexure bending (Van der Beek and Cloething, 1992).

SEISMITES

The seismites observed are the sedimentary expression of seismic activity related to faults. One approach for checking the seismic origin of a deformational structure is to demonstrate the relationship between the fracture mechanisms and the seismite trigger mechanism. The rocks are subjected to stress fields that produce faults, which may be accompanied by seismic activity. If seismic activity is continuous, earthquakes can produce deformations in soft sediments. The seismites are generated under the same regional or local stress field that originates the fault slip which can trigger earthquakes. Therefore, the origin of the seismites will be

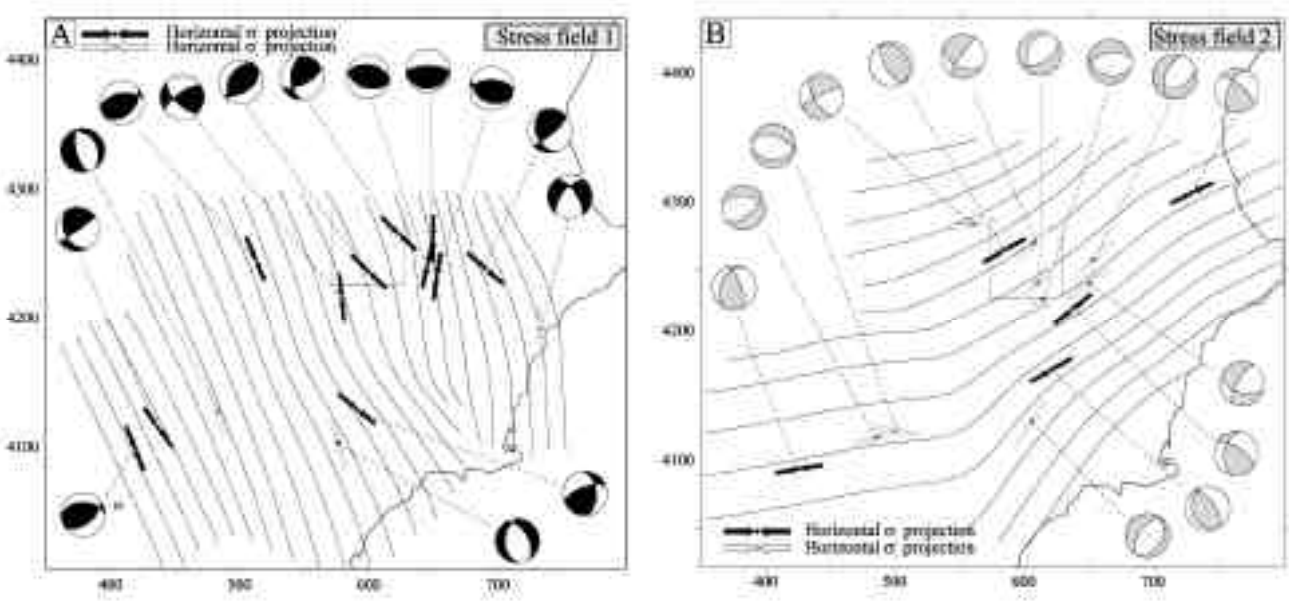

Figure 8. Earthquake focal mechanisms calculated by population analysis. Trajectories of σ_{HMAX} of: A) stress field 1 and B) stress field 2. Boxed area encloses the study area.

Figura 8. Mecanismos focales de terremotos calculados mediante análisis poblacional. Trayectorias de σ_{HMAX} de: A) campo de esfuerzos 1 y B) campo de esfuerzos 2. El área enmarcada representa el área de estudio.

constrained by the stress field and the seismites will behave like a pure tectonic structure.

The effect of seismic shocks is recorded in a variety of ways in the sediments of deep lake environments and shallow marginal lake areas since the deposits show diverse physical properties, i. e. there are different responses to pore fluid pressure related to variable grain-size, and consequently there are different susceptibilities to deformation produced in most cases, by liquefaction and fluidization processes (Owen, 1996). We agree with Atkinson (1984), who considers M5 to be the lowest magnitude that can generate liquefaction given that earthquakes of M<5 do not last sufficiently long to produce liquefaction, which is in keeping with the findings of Audemard and De Santis (1991).

Deep lake deposits

In the basins studied, deep lacustrine facies consist mainly of diatomaceous, varve-like laminated sediments and marlstone turbidites. The diatom-rich laminites are characterized by great cohesion, considerable natural shear strength and high sensitivity (Grimm and Orange, 1997). This makes the laminites prone to extensive brittle, plastic and/or fluid deformation when subjected to mechanical deformation. The following paragraphs briefly describe the soft-sediment deformation structures recognized in this facies:

Loop bedding

Loop bedding consists of bundles of laminae that are sharply constricted at intervals with a morphology of loops or links of a chain. In the study area, loop bedding is fairly common in laminite sequences in the Híjar and Elche de la Sierra basins. Four main types of loops have been observed at this horizon (Calvo et al., 1998) (simple and complex loops with subcategories which embrace folded to microfaulted packages of laminae). The thickness of the loop bedded layers ranges typically from 8 to 15 mm and the loops end laterally at decimetric intervals. The measured orientations of the loop axes are distributed according to two roughly perpendicular directions: 005 (predominant) and 105 (subordinate).

Loop bedding in laminite sequences have been interpreted as a result of stretching of unlithified to progressively more lithified laminated sediments in

response to successive minor seismic shocks related to the slow movement of extensional faults (Calvo et al., 1998) (Fig. 9).

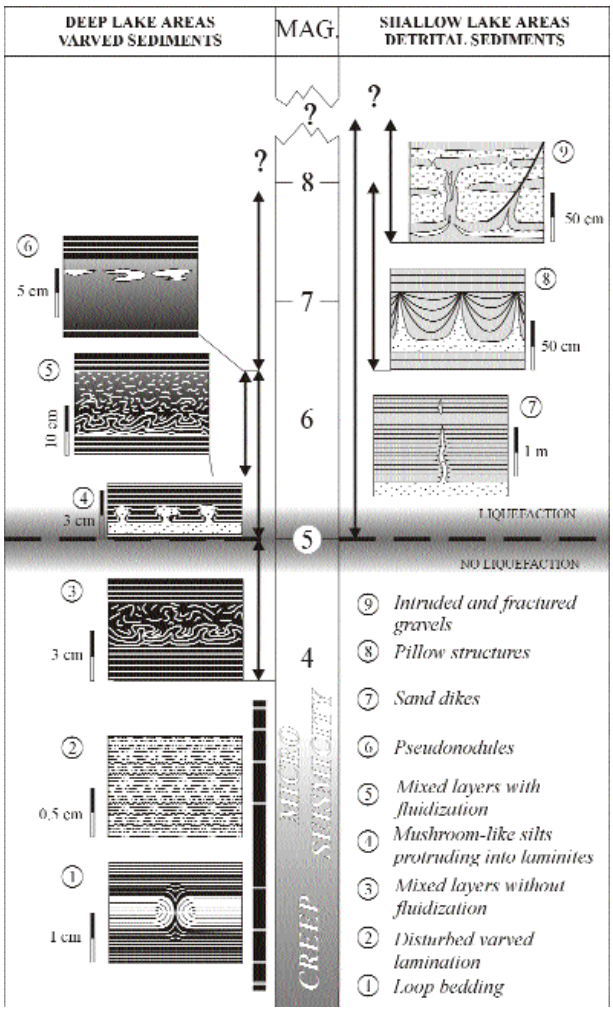

Figure 9. Summarized sketch of several seismite types observed in the Neogene lacustrine basins of the Prebetic Zone. Magnitudes at which the different seismites form. Lower limit (M > 5-5.5) for liquefaction is based on Atkinson (1984). Seismites occurring in deep and shallow lake deposits are sketched in separate columns. Modified from Rodríguez-Pascua et al. (2000).

Figura 9. Esquema resumen de los diferentes tipos de sismitas reconocidas en las cuencas neógneas del Prebético de Albacete. Se han representado los intervalos de magnitud en los que se ha interpretado se pueden formar estas estructuras. El límite inferior a la licuefacción (M > 5-5,5) está basado en Atkinson (1984). Se han separado en sendas columnas las sismitas formadas en medios someros y profundos. Modificada de Rodríguez-Pascua et al. (2000).

Disturbed varved lamination

This structure, which is characteristic of laminite sequences, consists of packages of diatomite laminae that display irregular thinning and thickening without losing their lateral geometric continuity. The disorganization of the laminae is recognized both in outcrop and in thin-sections. Some micro-faults are locally observed within the laminites (ductile-brittle behavior of the sediment). This type of deformational structure was mainly identified in the lacustrine succession of the Híjar basin.

We attribute the deformation to a continuous, slow movement of the faults limiting the basin, resulting in micro-seismic shocks of higher magnitudes than those causing loop bedding in laminites (Fig. 9).

Mixed layers

The term "mixed layer" was first used by Marco and Agnon (1995). The origin of this seismite is related to the activity of faults which generates moderate to high magnitude seismic shocks. Examples of mixed layers were observed at several levels of the late Miocene succession in Híjar, El Cenajo and Elche de la Sierra basins. They are normally associated with varve-like, laminite units where four horizons may be differentiated from bottom to top: i) basal undisturbed laminite bed, ii) folded laminites, iii) fractured and fragmented laminites, and iv) graded layer from fragment-supported to matrix-supported texture. The thickness of the sequence of the mixed layer and its folded lower contact ranges from 4 to 10 cm. The top of the mixed layer is overlain by horizontally laminated sediments in sharp contact (Rodríguez-Pascua et al., 2000).

In agreement with these observations, the sequence showing the "mixed layer" can be interpreted as the result of a single seismic event promoting downward migration of the deformation through a cohesive sediment (Marco and Agnon, 1995). Earthquake magnitudes M>5 are assumed to be necessary for triggering liquefaction of laminite sequences (Fig. 9).

Mushroom-like silts protruding into laminites

This structure consists of small diapir-like morphologies made up of silt-size sediment which intrudes and deforms overlying laminites. They were

observed at several horizons toward the upper part of the lacustrine succession of the El Cenajo basin. The mushroom-like structures are present with a horizontal spacing of 10-15 cm throughout the beds and show widths of 1-2 cm and heights of up to 0.5 cm. In plan view, the protruding silts show linear to slightly sinuous ridges which locally open up into separate branches (NE-SW trend, locally parallel to σ_{HMAX} NE-SW) (Rodríguez-Pascua et al., 2000).

The liquefaction of marlstone interbedded with laminites resulting in mushroom-like structures could take place at slightly lower earthquake magnitudes (M>5, Hempton and Dewey, 1983) (Fig. 9).

Pseudonodules

In the study area, pseudonodules, a type of deformational structure consisting of isolated masses of sediment of various morphologies (saucer-like, detached pillows, bolsters, etc.) embedded in an underlying deposit of contrasted density (Allen, 1982) are present in marlstone facies alternating with laminites. The pseudonodules occur as a single, laterally extensive row of 1 cm thick, white diatomaceous marlstone bodies which are interspersed in denser marlstone at the top of a turbidite bed which is overlain by laminites (Fig. 9). Pseudonodules, which are a classic deformational structure analyzed in detail by Kuenen (1958), would require earthquake magnitudes probably exceeding 6.5 for their formation (Rodríguez-Pascua et al., 2000) (Fig. 9).

Shallow marginal lake deposits

Seismites observed in shallow lake deposits have been interpreted in all the cases as resulting from the liquefaction of coarser-grained (sands, locally gravels), less cohesive deposits, where natural shear strength is considerably reduced compared with the laminites and associated sediments. These structures are developed in shallow-lake facies, especially in terrigenous fan-delta facies and turbidite limestones.

Sand dikes

In the lacustrine formations of the Prebetic area, sand dikes were observed at several levels of the stratigraphic succession, especially in the Las Minas basin. A network of dikes made up of major sand intrusions with laterally

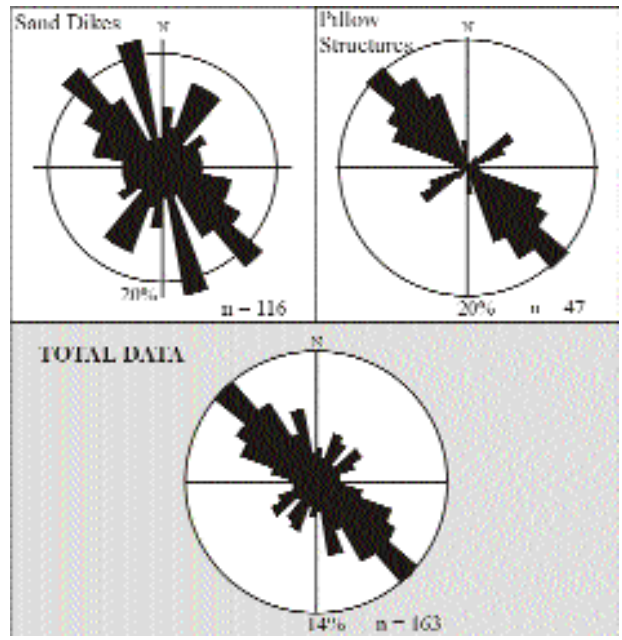

Figure 10. Rose diagrams of trend of sand dikes planes, fold axes of pillow structures and of total liquefaction structures.

Figura 10. Rosas de direcciones de planos de diques de arenas, estructuras en almohadilla y datos totales.

linked dikes is commonly observed. The major dikes bend the intruded layers upward whilst layers crossed by the subordinate dikes display opposite bending directions. The sand dikes show two main directions: N150E (major dikes) and N060E (subordinate), which are perpendicular (Fig. 10). In most cases, the dikes are vertical in cross-section (Rodríguez-Pascua et al., 2000).

The upward movement of the sand is supported by the fact that the major dikes are rooted in a basal sand bed and by the upward bending of the layers confining the sand dike. In contrast, the subordinate dikes resulted from the lateral flow of the sand perpendicular to the major dikes. Sand dikes occurring in lacustrine and fluvial deposits have been attributed to earthquakes of magnitudes ranging from 5 to 8 (Audemard and De Santis, 1991; Obermaier et al., 1993) (Fig. 9).

Pillow structures

This type of structure is mainly present in the Las Minas basin. The pillows occur at fairly regular intervals across single layered sand beds forming a series of laterally connected synforms and antiforms. In plan view,

the axes of the pillows show two directions: N150E (predominant) and N060E (subordinate) (Rodríguez-Pascua et al., 2000) (Fig. 10).

We postulate that the pillow structures observed in the lacustrine deposits of the Prebetic area were seismically induced given that the sediments in which they occur do not show significant density variations and are not covered with lithologies that could cause sudden overloading. A range of earthquake magnitudes (6.5-8) has been deduced for pillow structures developed in littoral marine, deltaic or fluvial deposits (Cojan and Thiry, 1992; Guiraud and Plaziat, 1993; Obermaier et al., 1993) (Fig. 9).

Intruded and fractured gravels

The occurrence of this structure is restricted to the uppermost part of the section in the Híjar basin. The deformation affects gravels and sands deposited in a subaqueous fan delta environment (Jiménez Sánchez, 1997). The beds are characterized by the presence of narrow antiforms and associated fractures through which underlying gravel and sand beds intrude upward up to 1.5 m. The fractures are both normal and reverse. These faults show two directions: N110E (predominant, always corresponding to normal fracture planes) and N010E (subordinate).

As pointed out by Guiraud and Plaziat (1993) and Obermeier et al. (1993), the magnitudes of the earthquakes inducing the formation of this type of deformational structure are necessarily high. Under this assumption, the intruded and fractured gravels reflect deformation under both brittle and ductile conditions triggered by strong seismic shocks (M>7.5) (Fig. 9).

INFERENCES FROM PALEOSEISMIC ANALYSIS

Relationship between stress field and seismites

A close relationship between the described structures and the tectonic pattern of the region is supported by the coincidence of the main orientation modes shown by the deformational structures and those of the major faults bounding the basins. The regional stress field that structured the area from the late Miocene to date is characterized by an average orientation of σ_{HMAX} toward NW-SE, as determined by kinematic and dynamic analyses (Martín Velázquez et al., 1998; Rodríguez Pascua, 1998). The orientations of the seismites, especially those measured in sand dikes (n = 116), intruded and fractured gravels (n = 28), pillow structures (n = 52), mushroom-like silts protruding into laminites (n = 41) and loop bedding (n = 62) are similar regardless of the measured deformational structure: the main mode of the orientation is NW-SE and the subordinate mode is NE-SW (Rodríguez-Pascua et al., 2000). This quasi-perpendicular distribution of the orientations reflects a radial trend of the tensional stresses that controlled the formation of the seismites. This distribution is in turn coincident with the regional tectonic stress field (Figs. 7 and 8).

Paleoearthquake influence radius

According to a number of authors (Obermeier et al., 1991; Moretti et al., 1995; Audemard and De Santis, 1991) liquefaction can be generated in an epicentral radius that oscillates between 25 km (M>5 to 5.7), 40 km (M>6), 70 (M>7) and 100 km (M>7.5) (Fig. 11A). Galli and Ferrelli (1995) made a compilation of 12,880 liquefaction structures generated by 159 earthquakes. Ninety five percent of these structures were generated at a distance of less than 25 km from the epicentral area (Fig. 11B). Bearing this in mind, the liquefaction structures observed in the lacustrine deposits were generated by earthquakes in the proximity and, therefore, the structures were related to the faults bounding the basins or crossing the study area.

Earthquake recurrence intervals

Based on the annual character of the laminated sediments in North American reservoirs, Sims (1975) dated the seismites in these artificial basins. Furthermore, the seismites were correlated with historical earthquakes. Doig (1991) estimated earthquake recurrence intervals in lacustrine sediments by radiometric dating techniques (^{14}C). Earthquake recurrence intervals were achieved by deformational structures in glacier varved sediments (Beck et al., 1996). Haczewski (1996) determined seismic patterns from studies on the chronostratigraphy and space-temporary disposition of deformational structures in old sediments (Oligocene pelagic limestones in the Polish Carpaths). These limestones contain varves resulting from annual sedimentation, and can be used for relative dating. The laminae pairs correspond to non-glacial

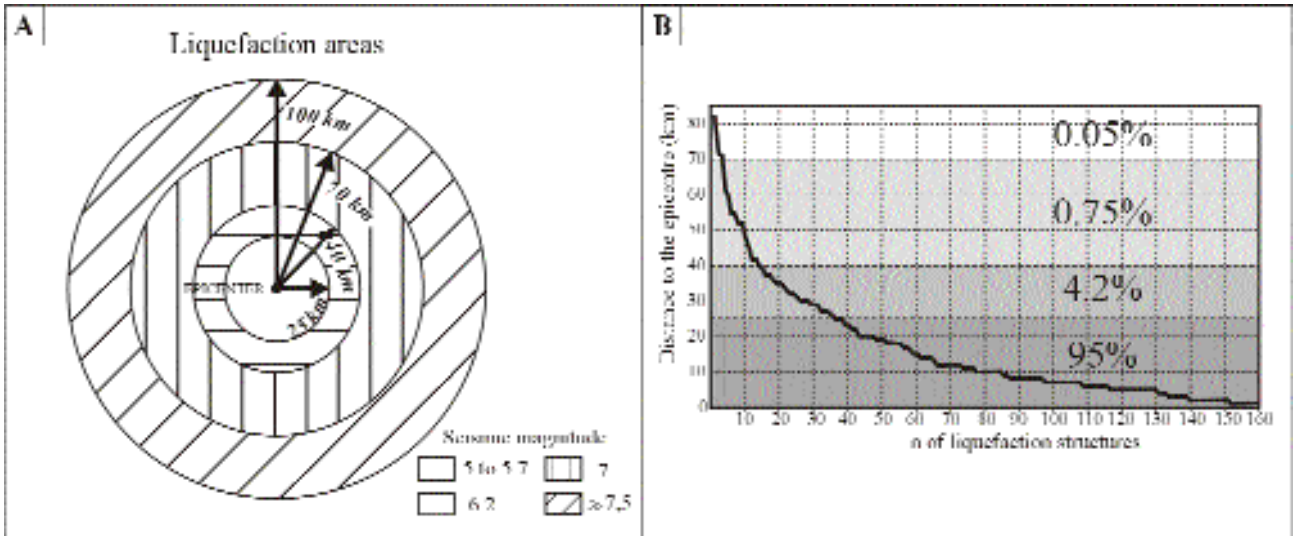

Figure 11. A) Liquefaction influence radius vs. seismic magnitude (Obermeier et al., 1991; Moretti et al., 1995; Audemard and De Santis, 1991) and B) percentage of liquefaction structures and liquefaction influence radius of earthquakes (modified from Galli and Ferrelli, 1995).

Figura 11. A) Radio de influencia de fenómenos de licuefacción con respecto a la magnitud sísmica (Obermeier et al., 1991; Moretti et al., 1995; Audemard y De Santis, 1991) y B) Porcentaje de estructuras de licuefacción generadas y radios de influencia de licuefacciones generadas por terremotos (modificada de Galli y Ferrelli, 1995).

varves and have an annual character. The light, carbonate-rich laminae precipitated at times of increased water temperature, i.e. during late spring and summer, whereas the dark, organic-rich laminae containing numerous diatom frustules formed in late autumn and winter (Kelts and Hsü, 1978; Anderson and Dean, 1988).

We used the mixed layers as paleoseismic indicators to calculate the paleoearthquake recurrence intervals. Mixed-layers were developed only in finely laminated sediments deposited subaqueously. These structures were first reported by Marco et al. (1994) in varved sediments of lake Lisan (Pleistocene) in the Dead sea (the Middle East). In these deposits, mixed-layers are associated with synsedimentary normal faults. Marco and Agnon (1995) suggested that the mixed layers were triggered by seismic shaking of magnitudes equal or higher than 5.5. No evidence for lateral displacement was found, i. e. sliding of the reworked laminite. Three zones characterized by distinctive styles of deformation can be distinguished: an uppermost fluidification zone, an intermediate zone of ductile-fragile deformation (break age and fragmentation of varves), and a lower ductile deformation zone (folding of varves), which overlies non-deformed laminae.

A set of successive deformational stages can usually be deduced from the evolutionary stages of mixed-layers. In the early stages of evolution of mixed layers triggered by earthquakes, a folding band of the laminated sediment surface is generated. During the shaking, this zone can no longer accommodate the deformation by folding and will begin to fracture. The folded area, which is limited to the inferior level, descends. The next deformational stage results in fluidification into the faulting area; the lower folded area fragments and descends into a lower level. In this way, the deformation progresses step by step from the top to the bottom laminate layer during the earthquake. Deformation increases from the top to the bottom of the mixed layer. But the deformation does not continue indefinitely at deeper stratigraphic levels since it is conditioned by the increase in lithification with depth. The laminites are not affected by cyclic shear stresses on the surface where the lithification prevents deformation. The most important mixed layers observed in the studied sedimentary logs did not exceed 15 cm. Fluidification is related to seismic shocks of magnitudes between 5-5.5 (Seed and Idriss, 1982; Atkinson, 1984; Thorson et al., 1986; Scott and Price, 1988; Audemard and de Santis, 1991; Cojan and Thiry, 1992; Papadopoulos and Lefkopoulos, 1993; Dugue, 1995; Marco and Agnon, 1995). These stages are conditioned

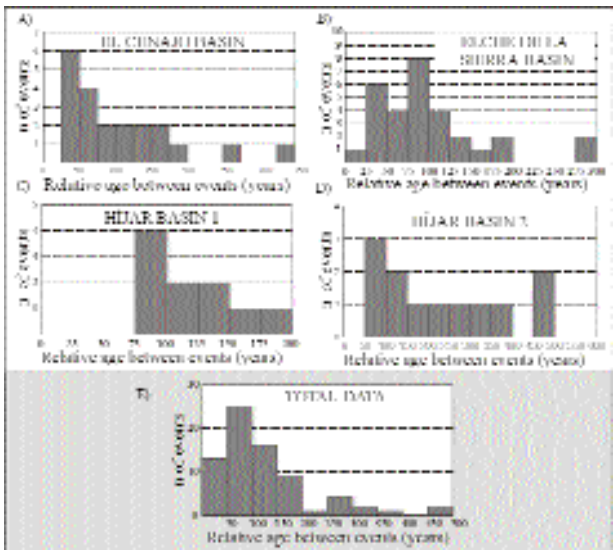

Figure 12. Paleoearthquake recurrence histograms calculated in the basins studied by varved sediment dating.

Figura 12. Histogramas de recurrencia de paleoterremotos calculados mediante datación relativa con sedimentos varvados en las cuencas estudiadas.

by the earthquake duration. Nevertheless, it is not easy to ascertain whether a structure has been generated by a large brief earthquake or by one with smaller energy and a longer duration. Empirical studies carried out in Italy (Galli and Ferreli, 1995) have registered 12,880 liquefaction structures generated by 158 earthquakes (historical and instrumental). Ninety-five percent of these structures were generated within a radius of less than 25 km from the epicenters of shallow earthquakes. In the External Betic area, this radius of influence was used to determine the extension of the area that underwent liquefaction. The seismites were generated close to the epicenters.

We used the varve-like sediments in deep lacustrine deposits as a relative dating method, and mixed layers as paleoseismic indicators. The earthquake recurrence intervals were calculated by detailed logs in the basins of Híjar (119±33 yr and 250±150 yr, with fault creep movements), El Cenajo (111±82 yr) and Elche de la Sierra (102±65 yr). The mean recurrence interval is 129±98 yr recorded in 9446 years with 73 dated events, one maximum interval of 454 years and one minimum interval of 23 years (Fig. 12). The mean estimated magnitude value is 5.1. In the Híjar basin, the sediments are affected by triaxial extensional stress that generated boudinage in accordance with a chocolate tablet pattern (Ramsay and Huber, 1983), resulting in well developed loop bedding (Calvo et al., 1998). These structures have been attributed to creep movements of normal faults that limit the basin (Calvo et al., 1998). The largest recurrence determined from these sediments (250 years) can be due to a higher rate of ductile (not seismic) deformation of the faults bounding the basin, which could result in a delay of the larger earthquakes.

The "b" value

We analyzed mixed layer structures in laminated beds in order to obtain the "b" value in the stratigraphic record. To this end, detailed logs of the laminite deposits were made. Assuming that the thickness of a mixed layer reflects the magnitude of the deformational force leading to the formation of seismites, the paleoseismic data must obey an exponential expression such as the Gutenberg-

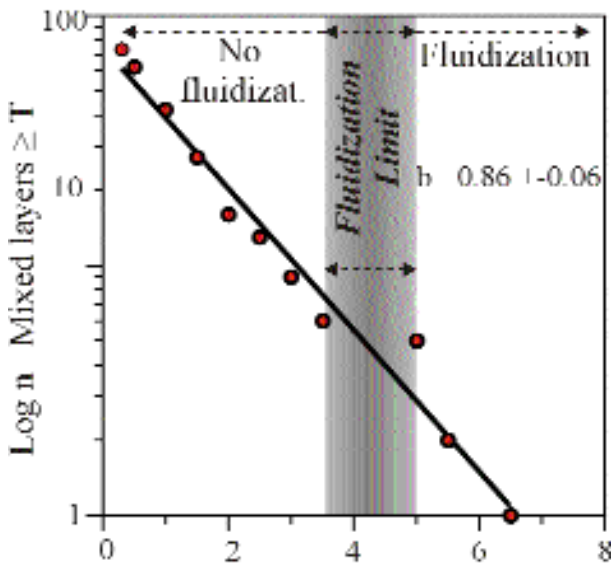

Figure 13. Semilogarithmic graphic plot of the accumulated number of events vs. magnitude and "b" value (the Gutenberg-Richter relationship) of paleoseismic data from mixed layers located in the Híjar, El Cenajo and Elche de la Sierra basins (relationship between mixed layer thickness and seismic magnitude).

Figura 13. Representación en una gráfica semilogarítmica del número acumulado de eventos frente a la magnitud y valor del parámetro "b" (ley de Gutenberg-Richter) de los datos paleosísmicos extraídos de las cuencas de Híjar, El Cenajo y Elche de la Sierra (relación entre la potencia de los niveles de mezcla y la magnitud sísmica).

Richter relationship. The fact that the palaeoseismic data set obeys the Gutenberg-Richter relationship suggests that there is a level of organization of earthquake size with respect to the time scale. This appears throughout the seismic deformational structures (mixed-layers) which are distributed as an instrumental seismic data set. This exponential relation was determined for all mixed layers (73 events) at Híjar, El Cenajo and Elche de la Sierra basins throughout the late Miocene (dated in a relative time scale) by adjusting data plotted by minimum squares. The "b" value calculated from such paleoseismic data is 0.86±0.06 (Fig. 13).

A relationship can be established between the mixed layer thickness and the earthquake magnitude by means of the Gutenberg-Richter relationship and the liquefaction limit of sediments (M>5-5.5). After plotting the data (number of events versus thickness) in a log-normal plot, the limit values of fluidization are represented on the graph. These limit values are close to those of the mixed layer thicknesses with incipient fluidization (magnitude 5) and to the values of thicknesses where the fluidization is a well-developed phenomenon, resulting from 5.5 magnitude earthquakes. Therefore, approximate values of the earthquake magnitude could be extrapolated to the rest of the mixed layers. Using mixed layers, an average magnitude of 4.2 is obtained from paleoseismic data, with a minimum magnitude of 3.7 and maximum magnitude of 6.1.

The area where the seismic data were selected is located between 0° and -4° longitude and 40° and 37° latitude. This is the maximum radius (100 km) in which liquefaction processes could be registered for earthquakes of M>8 (Moretti et al., 1995) (Fig. 14A). The instrumental seismicity shows a "b" value close to 0.86 (Fig. 14B) in agreement with that obtained from paleoseismic analysis. This value has a good degree of confidence according to Lee and Stewart (1981), who fixed limits between 0.6 and 1.2 for regional seismicity. Following Gutenberg-Richter (1956), the "b" value 0.89 used for measuring the regional seismicity approaches the "b" value obtained in the area studied (Fig. 13). These results are consistent with those obtained by a number of authors in the Betic chain (Karnik, 1971; Hatzfeld, 1978; De Miguel et al., 1983; García Dueñas et al., 1984; Vidal et al., 1984; Sanz de Galdeano and López Casado, 1988; Buforn et al., 1988; López Casado et al., 1995; Camacho and Alonso Chaves, 1997).

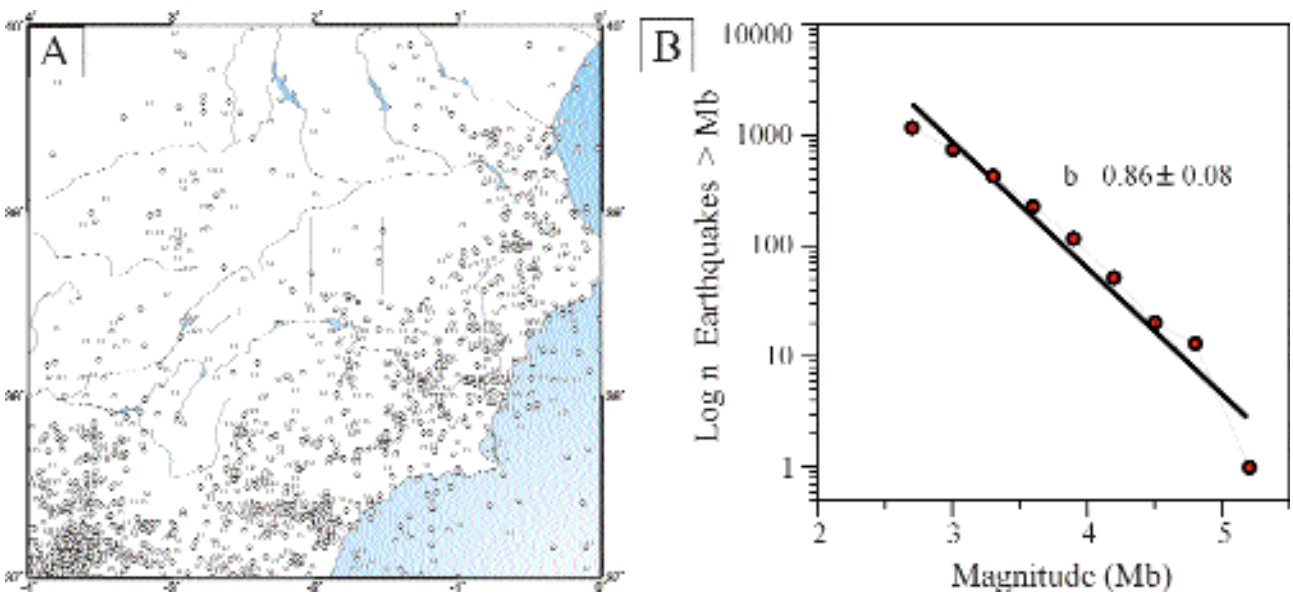

Figure 14. A) Epicentral location of instrumental seismicity (longitude: 0º to -4º; latitude: 37º to 40º) and B) semilogarithmic graphic plot of the accumulated number of events vs. magnitude and "b" value of seismic data.

Figura 14. A) Proyección epicentral de la sismicidad instrumental (longitud: 0º a -4º; latitud: 37º a 40º) y B) gráfica semilogarítmica del número acumulado de eventos frente a la magnitud y valor del parámetro "b" (ley de Gutenberg-Richter) para la sismicidad instrumental.

CONCLUSIONS

The analysis of lacustrine sediments considered as a "paleoseismograph", improves our understanding of seismic processes. Seismite formation in lacustrine successions was constrained by fault movements closely controlled by the regional stress field throughout the late Miocene. The orientations of the seismites (sand dikes, intruded and fractured gravels, pillow structures, mushroom-like silts protruding into laminites and loop bedding) are systematically consistent with the stress field trends. The main orientation is NW-SE and the subordinate one is NE-SW. This represents a link between tectonics and seismites given that the stress and deformation fields that structured the area also affected the sediments during their deposition. This suggests that the stresses responsible for the occurrence of earthquakes constrained the formation of seismites. Moreover, seismites can be used as fossil-magnitude indicators. The liquefaction structures were generated by adjacent earthquakes (epicentral radius less than 25 km), with a M>5.5. Therefore, these earthquakes were caused by the faults bounding the basins or crossing the studied area.

The earthquake recurrence intervals calculated in the basins of Híjar (119±33 yr and 250±150 yr with fault creep movements), El Cenajo (111±82 yr) and Elche de la Sierra (102±65 yr) were inferred from relative dating of mixed layers in laminite sediments. The average earthquake recurrence estimated for the different basins is 129±98 yr with an estimated average earthquake magnitude of 5.1. The analyzed sediments represent a total record of 9446 years, from which 73 events, with magnitudes ranging from 3.7 to 6.1, were dated. In the Híjar basin the sediments were affected by triaxial extensional stress related to creep movements of normal faults bounding the basins. The largest recurrence deviation of 150 years can be due to a higher rate of ductile deformation (not seismic) by the faults bounding the basin, which could result in delaying bigger earthquakes.

The paleoseismological and seismological data obey the Gutenberg-Richter relationship for magnitude values, showing a similar "b" value (close to 0.86). The "b" values obtained by other authors in different areas of the Betic chain are very similar to those calculated in this paper. This indicates a uniformity of the regional seismicity of the Betic chain for different areas within the same time interval, suggesting that the seismic conditions have not changed substantially since the late Miocene.

ACKNOWLEDGEMENTS

We thank P. Santanach and E. Masana for editing this monograph. We are indebted to S. Martín Velázquez, S. Jiménez Sánchez and D. Gómez Gras, who helped with the field work. We also thank Ll. Cabrera and A. Estévez for their invaluable comments on the content of the paper. Financial support from the "Consejo de Seguridad Nuclear" of Spain and the CICYT project AMB 94-0994 is gratefully acknowledged.

REFERENCES

Allen, J.R.L., 1982. Sedimentary Structures, Vol. II. Developments in Sedimentology, 30B, Amsterdam, Elsevier Publ. Co., 663 p.

Alvaro, M.G., Argüeso, J.M., Elizaga, E., 1975. La estructura del borde prebético de la zona de Alcaraz (Provincia de Albacete, España). Bol. Geol. Min., 86, 467-477.

Anderson, R.Y., Dean, W.E., 1988. Lacustrine varve formation through time. Palaeogeogr., Palaeoclim., Palaeoecol., 62, 215-235.

Angelier, J., Mechler, P., 1977. Sur une méthode graphique de recherche des contraintes principales également utilisable en tectonique et en séismologie: la méthode des dièdres droits. Bull. Soc. géol. France, 7, 1309-1318.

Atkinson, G., 1984. Simple computation of liquefaction probability for seismic hazard applications. Earthquake Spectra, 1(1), 107-123.

Audemard, A., De Santis, F., 1991. Survey of liquefaction structures induced by recent moderate earthquakes. Bull. Inter. Assoc. Eng. Geol., 44, 5-16.

Beck, C., Frédéric, M., Chapron, E., Van Rensbergen, P., De Batist, M., 1996. Enhanced seismicity in the early post-glacial period: evidence from the Post-Würm sediments of Lake Annency, northwestern Alps. Jour. Geodynamics, 22(1/2), 155-171.

Bellanca, A., Calvo, J.P., Censi, P., Elízaga, E., Neri, R., 1989. Evolución of lacustrine diatomite carbonate cycles of Miocene age, SE Spain: petrology and isotope geochemistry. Jour. Sed. Petrol., 59, 45-52.

Bellon, H., Bizon, G., Calvo, J.P., Elizaga, E., Gaudant, J., López Martínez, N., 1981. Le volcan du Cerro del Monagrillo (Province de Murcia): âge radiométrique et corrélations avec les sédiments néogènes du basin de Hellín (Espagne). C. R. Acad. Sci. París, 292, 1035-1038.

Bott, M.H.P., 1959. The mechanism of oblique-slip faulting. Geol. Mag., 96, 109-117.

Buforn, E., Udías, A., Colombás, M.A., 1988. Seismicity, source mechanisms and tectonics of the Azores-Gibraltar plate boundary. Tectonophysics, 152, 89-118.

Calvo, J.P., Elízaga, E., López Martínez, N., Robles, F., Usera, J., 1978. El Mioceno superior continental del Prebético Ex-

terno: Evolución del Estrecho Norbético. Bol. Geol. Min., 89, 407-426.

Calvo, J.P., Elízaga, E., 1987. Diatomite deposits in South-eastern Spain: geologic and economic aspects. Ann. Inst. Geol. Publ. Hungar., 70, 537-543.

Calvo, J.P., Elízaga, E., 1994. The Cenajo and Las Minas-Camarillas basins (Miocene), southeastern Spain. In E. Gierlowski-Kordesch, K. Kelts, (eds.), Global Inventory of Lake Systems, Cambridge, University Press, 319-324.

Calvo, J.P., Rodríguez-Pascua, M.A., Martín-Velázquez, Jiménez, S., De Vicente, G., 1998. Microdeformation of lacustrine laminite sequences from Late Miocene formations of SE Spain: an interpretation of loop bedding. Sedimentology, 45, 279-292.

Calvo, J.P., Gómez-Gras, D., Alonso-Zarza, A.M., Jiménez, S., 2000. Architecture of a bench-type carbonate lake margin and its relation to fluvially dominated deltas, Las Minas Basin, Upper Miocene, Spain. Jour. Sed. Res., 70(1), 240-254.

Camacho, M.A., Alonso-Chaves, M., 1997. Sismicidad en el límite de placas entre Eurasia y África al SW de Iberia, desde 1984 a 1994. Geogaceta, 21, 51-54.

Cojan, I., Thiry, M., 1992. Seismically induced deformation structures in Oligocene shallow-marine and eolian coastal sands (Paris Basin). Tectonophysics, 206, 79-89.

Collinson, J., 1994. Sedimentary deformational structures. In A. Maltman (ed.), The geological deformation of sediments, London, Chapman & Hall, 95-125.

De Miguel, F., Vidal, F., Alguacil, G., Guirao, J.M., Olivares, G., 1983. Red sísmica de la Universidad de Granada. Seminario sobre Simicidad y Riesgo Sísmico del Área Ibero-Mogrebí. Córdoba, 7-11.

De Vicente, G., 1988. Análisis Poblacional de Fallas. El sector de enlace Sistema Central-Cordillera Ibérica. Tesis Doctoral, Univ. Complutense de Madrid, Publ. Univ. Compl. Madrid., 317 p.

Delvaux, D., 1993. The Tensor program for paleostress reconstruction: examples from the east African and the Baikal rift zones. Terra Abstracts, 5, 1, 216 .

Delvaux, D., Levi, K., Kajara, R., Sarota, J., 1992. Cenozoic paleostress and kinematic evolution of the Rukwa. North Malawi rift valley (East African Rift System). Bull. Cent. Rech. Explor. Prod. Elf- Aquit., 16(2), 283-406.

Doig. R., 1991. Effects of strong seismic shaking in lake sediments, and earthquake recurrence interval, Témiscaming, Quebec. Can. Jour. Earth Sci., 28, 1349-1352.

Dugué, O., 1995. Séismites dans le Jurasique supérieur du Bassin anglo-parisien (Normandie, Oxfordien supérieur, Calcaire gréseux de Hennequeville). Sedim. Geol., 99, 73-93.

Elízaga, E., 1994. Análisis de las facies y petrología de los depósitos lacustres de edad Neógeno superior. Albacete. España. Albacete, Instituto de Estudios Albacetenses, I, 74, 216 p.

Elízaga, E., Calvo, J.P., 1988. Evolución sedimentaria de las cuencas lacustres neógenas de la Zona Prebética (Albacete, España). Relación, posición y efectos del vulcanismo durante la evolución. Bol. Geol. Min., 99, 837-846.

Fuster, J.M., Gastesi, P., Sagredo, J., Fermoso, M.L., 1967. Las rocas lamproíticas del SE de España. Estudios Geol., 23, 35-69.

Galli, P., Ferreli, M., 1995. A metholological approach for historical liquefaction research. In L. Serva, D.B. Slemmons (eds.), Perspectives in Paleoseismology, Assoc. Eng. Geol., Spec. Pub., 6, 35-48.

García-Dueñas, V., Sanz de Galdeano, C., De Miguel, F., Vidal, F., 1984. Neotectónica y sismicidad en las Cordilleras Béticas: una revisión de resultados. Energía Nuclear (J.E.N.), 28(149-150), 231-248.

Giner, J.L., 1996. Análisis sismotectónico y neotectónico en el sector centro-oriental de la Cuenca del Tajo. Tesis Doctoral. Univ. Complutense de Madrid, 268 p.

Grimm. K.A., Orange, D.L., 1997. Synsedimentary fracturing, fluid migration, and subaqueous mass wasting: intrastratal microfractured zones in laminated diatomaceous sediments, Miocene Monterey Formation, California, U.S.A. Jour. Sediment. Research, 67, 601-613.

Guiraud, M., Plaziat, J.C., 1993. Seismites in the fluviatile Bima sandstones: identification of paleoseisms and discussion of their magnitudes in a Cretaceous synsedimentary strike-slip basin (Upper Benue, Nigeria). Tectonophysics, 225, 493-522.

Gutenberg, B., Richter, C.F., 1956. Magnitude and energy of earthquakes. Ann. Geofis., 9, 1-15.

Haczewski, G., 1996. Oligocene laminated limestones as a High-resolution correlator of paleoseismicity, Polish Carpathians. In A.E.S. Kemp (ed.), Paleoclimatology and Palaeoceanography from laminated sediments. Geol. Soc., Spec. Pub., 116, 258-000.

Hatzfield, D., 1978. Étude sismotectonique de la zone de collision Ibéro-Maghrébine. Thèse Univ. de Grenoble, 281 p.

Hempton, M.R., Dewey, J.S., 1983. Earthquake-induced deformational structures in young lacustrine sediments, East Anatolian Fault, southeast Turkey. Tectonophysics, 98, T14-T17.

Jiménez Sánchez, S., 1997. Formación de depósitos diatomíticos en cuencas neógenas del sureste de la provincia de Albacete. Albacete, Instituto de Estudios Albacetenses, 154 p.

Karnik, V., 1971. Seismicity of the European area. Part 2. D. Dordrecht, Reidel Publis. Comp, 218 p.

Kelts, K., Hsü, K.J., 1978. Freshwater Carbonate Sedimentation. In A. Lerman (ed.), Lakes. Chemistry, Geology, Physics, New York, Springer-Verlag, 295-323.

Kuenen, P.H., 1958. Experiments in geology. Trans. Geol. Soc. of Glasgow, 23, 1-27.

Lee, J.C., Angelier, J., 1994. Paleostress trajectory maps based on the results of local determinations: the "lissage" program. Computers and Geosciences, 20(2), 161-191.

Lee, W.H.K., Stewart, S.W., 1981. Principes and applications of microearthquake networks. New York, Academic Press, 293 p.

López Casado, C., Sanz de Galdeano, C., Delgado, J., Peinado, M.A., 1995. The b parameter in the Betic Cordillera, Rif and nearby sectors. Relations with the tectonics of the region. Tectonophysics, 248, 277-292.

Marco, S., Agnon, A., Stein, M., Ron, H., 1994. A 50,000 continuous record of eathquakes and surface ruptures in the Lisan Formation, the Dead Sea Graben. U.S. Geol. Surv. Open-File Report, 94-568, 112-114.

Marco, S., Agnon, A., 1995. Prehistoric earthquake deformations near Masada, Dead Sea Graben. Geology, 23, 695-698.

Martín Velázquez, S., De Vicente, G., Rodríguez-Pascua, M.A., Calvo, J.P., 1998. Análisis dinámico del sistema de desgarres NO-SE del Prebético de Albacete. Rev. Soc. Geol. España, 11(3-4), 369-383.

Moretti, M., Pieri, P., Tropeano, M., Walsh, N., 1995. Tyrrhenian seismites in Bari Area (Murge-Apulian foreland). Atti dei Convegni Licenci, 122. Terremoti in Italia. Accademia Nazionale dei Lincei, 211-216.

Obermeier, S.F., Bleuer, N.R., Munson, C.A., Martin, P.J., McWilliams, K.M., Tabaczynski, D.A., Odum, J.K., Rubin, M., Eggert, D.L., 1991. Evidence of strong eathquake shaking in lower Wabash Valley from prehistoric liquefactions features. Science, 251, 1061-1063.

Obermaier, S.F., Martin, J.R., Frankel, A.D., Youd, T.L., Munson, P.J., Munson, C.A., Pond, E.C., 1993. Liquefaction evidence for one or more strong Holocene earthquakes in the Wabash Valley of southern Indiana and Illinois, with a preliminary estimate of magnitude. U.S. Geol. Surv. Prof. Paper, 1536, 27 p.

Owen, H.G., 1996. Experimental soft-sediment deformation: structures formed by the liquefaction of unconsolidated sands and some ancient examples. Sedimentology, 43, 279-293.

Papadopoulos, G. A., Lefkopoulos, G., 1993. Magnitude-distance relations for liquefaction in soil from earthquakes. Bull. Seismol. Soc. Amer., 83(3) 925-938.

Pegoraro, O., 1972. Application de la microtectonique à une étude de néotectonique. Le golfe Maliaque (Grèce centrale). Thèse IIIème cycle, U.S.T.L., Montpellier, 41 p.

Ramsay, J.G., Huber, M.I., 1983. The technics of modern structural geology, vol I strain analysis. London, Academic Press, 307 p.

Reches, Z., 1978. Analysis of faulting in three-dimensional strain fields. Tectonophysics, 47 (1-2), 109-129.

Reches, Z., 1983. Faulting of rocks in three-dimensional strain fields, II. Theoretical analysis. Tectonophysics, 95, 133-156.

Richi Lucci, F., 1995. Sedimentatological indicators of Paleoseismicity. In L. Serva, D.B. Slemmons (eds.), Perspectives in Paleoseismology. Assoc. Eng. Geol., Spec. Pub., 6, 7-18

Rodríguez Pascua, M.A., 1997. Paleosismicidad en Emplazamientos Nucleares. Estudio en relación con el cálculo de la peligrosidad sísmica. Consejo de Seguridad Nuclear, 286 p.

Rodríguez Pascua, M.A., 1998. Paleosismicidad y sismotectónica de las cuencas lacustres neógenas del Prebético de Albacete. Tesis Doctoral, Univ. Complutense de Madrid, 358 p.

Rodríguez Pascua, M.A., Calvo, J.P., De Vicente, G., Gómez Gras, D., 2000. Soft-sediment structures interpreted as seismites in lacustrine sediments of the Prebetic Zone, SE Spain, and their potential use as indicators of earthquake magnitudes during the Late Miocene. Sedim. Geol., 135, 117-135.

Sanz de Galdeano, C., López Casado, C., 1988. Fuentes sísmicas en el ámbito Bético-Rifeño. Rev. Geofís., 44, 175-198.

Sanz de Galdeano, C., Vera, J. A., 1991. Una propuesta de clasificación de las cuencas neógenas béticas. Acta Geol. Hisp., 26(3-4), 205-227.

Scott, B., Price, S., 1988. Earthquake-induced structures in young sediments. Tectonophysics, 147, 165-170.

Seed, H.B., Idriss, I.M., 1982. Ground motions and soil liquefaction during earthquakes. Berkeley, Earthquake Eng. Res. Inst., 134 p.

Seilacher, A., 1969. Fault graded beds interpreted as seismites. Sedimentology, 13, 155-159.

Sims, J.D., 1975. Determining earthquake recurrence intervals from deformational structures in young lacustrine sediments. Tectonophysics, 29, 141-152.

Thorson, R.M., Claiton, W.S., Seever, L., 1986. Geologic evidence for a large prehistoric earthquake in easthern of Conecticut. Geology, 14, 463-467.

Van der Beek, P. A., Cloething, G., 1992. Lithospheric flexure and the tectonic evolution of the Betic Cordilleras (SE Spain). Tectonophysics, 203, 325-344.

Vidal, F., De Miguel, F., Sanz de Galdeano, C., 1984. Neotectónica y sismicidad en la Depresión de Granada. Energía Nuclear (J.E.N.), 28(149-150), 267-275.